Precessional Instability in Binary Black Holes with Aligned Spins

Davide Gerosa, Michael Kesden, Richard O'Shaughnessy, Antoine Klein, Emanuele Berti, Ulrich Sperhake, and Daniele Trifirò

Precessional instability in binary black holes with aligned spins

Davide Gerosa,[1, *] Michael Kesden,[2, †] Richard O'Shaughnessy,[3, ‡] Antoine
Klein,[4, §] Emanuele Berti,[4, 5, 6, ¶] Ulrich Sperhake,[1, 4, 5, **] and Daniele Trifirò[4, 7, ††]

[1]*Department of Applied Mathematics and Theoretical Physics, Centre for Mathematical Sciences,
University of Cambridge, Wilberforce Road, Cambridge CB3 0WA, UK*
[2]*Department of Physics, The University of Texas at Dallas, Richardson, TX 75080, USA*
[3]*Center for Computational Relativity and Gravitation,
Rochester Institute of Technology, Rochester, NY 14623, USA*
[4]*Department of Physics and Astronomy, The University of Mississippi, University, MS 38677, USA*
[5]*California Institute of Technology, Pasadena, CA 91125, USA*
[6]*CENTRA, Departamento de Física, Instituto Superior Técnico,
Universidade de Lisboa, Avenida Rovisco Pais 1, 1049 Lisboa, Portugal*
[7]*Dipartimento di Fisica E. Fermi, Università di Pisa, Pisa 56127, Italy*
(Dated: September 1, 2015)

Binary black holes on quasicircular orbits with spins aligned with their orbital angular momentum have been testbeds for analytic and numerical relativity for decades, not least because symmetry ensures that such configurations are equilibrium solutions to the spin-precession equations. In this work, we show that these solutions can be unstable when the spin of the higher-mass black hole is aligned with the orbital angular momentum and the spin of the lower-mass black hole is anti-aligned. Spins in these configurations are unstable to precession to large misalignment when the binary separation r is between the values $r_{\mathrm{ud}\pm} = (\sqrt{\chi_1} \pm \sqrt{q\chi_2})^4 (1-q)^{-2} M$, where M is the total mass, $q \equiv m_2/m_1$ is the mass ratio, and χ_1 (χ_2) is the dimensionless spin of the more (less) massive black hole. This instability exists for a wide range of spin magnitudes and mass ratios and can occur in the strong-field regime near merger. We describe the origin and nature of the instability using recently developed analytical techniques to characterize fully generic spin precession. This instability provides a channel to circumvent astrophysical spin alignment at large binary separations, allowing significant spin precession prior to merger affecting both gravitational-wave and electromagnetic signatures of stellar-mass and supermassive binary black holes.

PACS numbers: 04.25.dg, 04.70.Bw, 04.30.-w

Introduction. – Black holes (BHs) have been observed in two distinct regimes: stellar-mass BHs ($5M_\odot \lesssim m \lesssim 100M_\odot$) accrete from companions in X-ray binaries [1–3], while supermassive BHs shine as quasars or active galactic nuclei (AGN) [4, 5]. Both types of BHs naturally occur in binaries: the massive stellar progenitors of stellar-mass BHs are typically formed in binaries, while supermassive BHs form binaries following the mergers of their host galaxies [6]. Gravitational radiation circularizes the orbits of these binaries [7] and causes them to inspiral and eventually merge, making them promising sources of gravitational waves (GWs) for current and future GW detectors [8–15]. The spins of these binary BHs need not be aligned with their orbital angular momentum: stellar-mass BHs may recoil during asymmetric collapses tilting their spins with respect to the orbital plane [16–18], while the initial orbital plane of supermassive BH binaries reflects that of their host galaxies and is thus independent of their spin. Gravitational effects alone will not align the BH spins with the orbital angular momentum [19, 20], but astrophysical mechanisms exist that drive the BH spins towards alignment in both regimes. The first BH to collapse in stellar-mass BH binaries may accrete in a disk from its as yet uncollapsed companion, while both members of a supermassive BH binary may accrete from a common circumbinary disk. Warps in these accretion disks can align the BH spins with the orbital angular momentum [21–23], but if the initial misalignment between the BH spin and accretion disk is greater than $90°$, the BH may instead be driven into anti-alignment [24].

Misaligned spins cause the orbital angular momentum to precess [25–27], modulating the emitted GWs [28]. Spin misalignment is both a blessing and a curse for GW data analysis: it increases the parameter space of templates needed to detect GWs via matched filtering but also breaks degeneracies between estimated parameters in detected events [29]. Misaligned spins at merger can generate large gravitational recoils [30–32], ejecting supermassive BHs from their host galaxies. Spin precession may also be responsible for the observed X-shaped morphology of AGN radio lobes [33, 34]. Given the importance of spin misalignment, it is worth investigating the robustness of aligned spin configurations. In the general case that the BHs have unequal masses, there are four distinct (anti-)aligned configurations, which we refer to as up-up, up-down, down-up, and down-down. The direction before (after) the hyphen describes the more (less) massive BH and up (down) implies (anti-)alignment of the spin with the orbital angular momentum. By symmetry, all four configurations are equilibrium solutions to the orbit-averaged spin-precession equations [27], but are
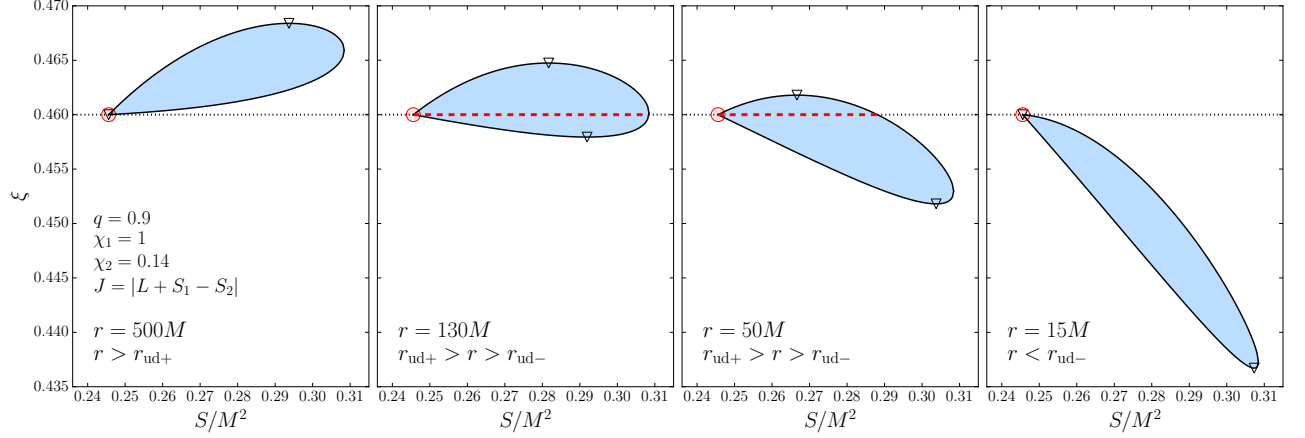
FIG. 1. Effective-potential loops $\xi_\pm(S)$ for binary BHs with mass ratio $q = 0.9$, dimensionless spins $\chi_1 = 1$, $\chi_2 = 0.14$, and total angular momentum $J = |L + S_1 - S_2|$, corresponding to the up-down configuration. For binary separations $r > r_{\rm ud+} \simeq 337M$ (left panel), the up-down configuration at $S_{\rm min}$ marked by a red circle is also a minimum (marked by the lower triangle). At intermediate separations $r_{\rm ud+} > r > r_{\rm ud-} \simeq 17M$ (middle panels), misaligned binaries with the same value of the conserved ξ exist along the dashed red line. Perturbations δJ, $\delta \xi$ will cause S to oscillate between the points $S_\pm$ where this line intersects the loop, making the up-down configuration unstable. For $r < r_{\rm ud-}$ (right panel), the up-down configuration is again a stable extremum, now a maximum (marked by the upper triangle). An animated version of this figure is available online at [35].

these solutions stable? To answer this question, we investigate how the configurations respond to perturbations of the spin directions using our recently developed approach for studying generically precessing systems [36, 37]. As we will demonstrate below, the up-down configuration is unstable for certain choices of binary parameters, with significant consequences for GW data analysis and astrophysics.

Generic spin precession. – Here we briefly summarize the approach to spin precession described in detail in [36, 37] using units where $G = c = 1$. Binary BHs with total mass $M = m_1 + m_2$, mass ratio $q = m_2/m_1 \leq 1$, symmetric mass ratio $\eta = q/(1+q)^2$, and spins $\mathbf{S}_i = \chi_i m_i^2 \hat{\mathbf{S}}_i$ evolve on three distinct timescales: the orbital time $t_{\rm orb} = (r^3/M)^{1/2}$ on which their separation $\mathbf{r}$ changes direction, the precession time $t_{\rm pre} = (t_{\rm orb}/\eta)(r/M)$ on which the spins and orbital angular momentum $\mathbf{L}$ change direction, and the radiation-reaction time $t_{\rm RR} = (t_{\rm orb}/\eta)(r/M)^{5/2}$ on which the magnitudes r and L decrease due to GW emission. The relative orientations of the spins are often specified by the two angles $\cos\theta_i = \hat{\mathbf{S}}_i \cdot \hat{\mathbf{L}}$ and the angle $\Delta\Phi$ between the projections of the two spins onto the orbital plane, all of which vary on $t_{\rm pre}$. The spin orientations can equivalently be specified by the magnitudes of the total spin $\mathbf{S} = \mathbf{S}_1 + \mathbf{S}_2$, the total angular momentum $\mathbf{J} = \mathbf{L} + \mathbf{S}$, and the projected effective spin [38, 39] $\xi \equiv M^{-2}[(1+q)\mathbf{S}_1 + (1+q^{-1})\mathbf{S}_2] \cdot \hat{\mathbf{L}}$. This specification has the advantage that only S evolves on $t_{\rm pre}$, while J evolves on $t_{\rm RR}$ and ξ is conserved throughout the post-Newtonian (PN) stage of the inspiral ($r \gtrsim 10M$) by orbit-averaged 2PN spin precession and 2.5PN radiation reaction [40]. On the precession time, the spin magnitude S simply oscillates back and forth

between the two roots $S_\pm$ of the equation $\xi = \xi_\pm(S)$, where

$$\xi_\pm(S) = \{(J^2 - L^2 - S^2)[S^2(1+q)^2 - (S_1^2 - S_2^2)(1 - q^2)]$$
$$\pm (1 - q^2)\sqrt{[J^2 - (L - S)^2][(L + S)^2 - J^2]}$$
$$\times \sqrt{[S^2 - (S_1 - S_2)^2][(S_1 + S_2)^2 - S^2]}\}/(4qM^2S^2L),$$
(1)

are the effective potentials for BH spin precession. Note that S is the only quantity on the right-hand side of Eq. (1) changing on $t_{\rm pre}$; in the absence of radiation reaction, the spins return to their initial relative orientation after a time $\tau(L, J, \xi)$ during which $\mathbf{L}$, $\mathbf{S}_1$, and $\mathbf{S}_2$ precess about $\mathbf{J}$ by an angle $\alpha(L, J, \xi)$. The two potentials $\xi_\pm(S)$ form a closed loop in the $S\xi$-plane, implying that the two roots $S_\pm$ coincide at the extrema $\xi_{\rm min,max}(L, J)$ of the loop. At these extrema, also known as spin-orbit resonances [19], S does not oscillate and $\mathbf{L}$, $\mathbf{S}_1$, and $\mathbf{S}_2$ all remain coplanar on the precession time.

Stability of aligned configurations. – We begin with the up-up and down-down configurations, for which $J = |L \pm (S_1 + S_2)|$, respectively. According to Eq. (1), the effective-potential loop reduces to a single point in this limit which is necessarily an extremum: S cannot oscillate consistent with conservation of J and ξ. Now consider the down-up (up-down) configurations for which $J = |L - S_1 + S_2|$ ($J = |L + S_1 - S_2|$). The effective-potential loop $\xi_\pm(S)$ encloses a nonzero area for these values of J, implying that oscillations in S are possible, except at the extrema $\xi_{\rm min,max}$. Since the spins are anti-aligned with each other in both configurations, S is minimized at $S_{\rm min} = |S_1 - S_2|$ and both configurations sit on the leftmost point of the loop, where $\xi_+(S)$ and
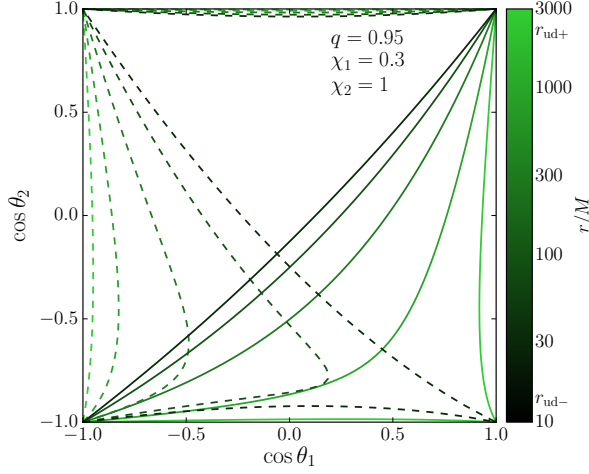
FIG. 2. The angles $\cos\theta_i = \hat{\mathbf{S}}_i \cdot \hat{\mathbf{L}}$ for spin-orbit resonances [extrema of $\xi_\pm(S)$] for BHs with $q = 0.95$, $\chi_1 = 0.3$, and $\chi_2 = 1$. The solid (dashed) curves indicate the $\Delta\Phi = 0$ (π) family and the five curves for each family correspond to binary separations $r/M = 3000, 720, 170, 40$, and 10. The up-down configuration (bottom right corner) belongs to the $\Delta\Phi = 0$ family for $r > r_{\mathrm{ud}+} \simeq 2149M$, to the $\Delta\Phi = \pi$ family for $r < r_{\mathrm{ud}-} \simeq 13M$, and is unstable for intermediate values $r_{\mathrm{ud}-} < r < r_{\mathrm{ud}+}$. An animated version of this figure is available online at [35].

FIG. 3. Precession-averaged radiation reaction dJ/dL as a function of J and ξ for binaries with $q = 0.8$, $\chi_1 = \chi_2 = 1$, and separation $r = 10M$ in the unstable region $r_{\mathrm{ud}-} < r < r_{\mathrm{ud}+}$. Spin-orbit resonances including the up-up, down-down, and down-up configurations are extrema of $\xi_\pm(S)$ and constitute the boundary of the allowed region. All four aligned configurations are maxima where $dJ/dL = 1$, but the unstable up-down configuration (shown in the inset) is a cusp. An animated version of this figure is available online at [35].

$\xi_-(S)$ coincide. Whether this point is also an extremum $\xi_{\mathrm{min,max}}$ depends on the slopes of these two functions at that point. Both slopes are always negative for the down-up configuration, implying that it is a maximum ξ_{max} and thus a spin-orbit resonance like the up-up and down-down configurations. At large binary separations r, the slopes of $\xi_\pm(S)$ are both positive for the up-down configuration, making it a minimum ξ_{min}. However, below $r_{\mathrm{ud}+}$ given by

$$r_{\mathrm{ud}\pm} = \frac{(\sqrt{\chi_1} \pm \sqrt{q\chi_2})^4}{(1-q)^2} M \;, \qquad (2)$$

the slope of $\xi_-(S)$ becomes negative and up-down is no longer an extremum of the effective-potential loop, as seen in Fig. 1. At separations below $r_{\mathrm{ud}-}$, the slope of $\xi_+(S)$ also becomes negative and up-down is again an extremum, this time a maximum ξ_{max}. Misaligned BHs with the *same* values of J and ξ as the up-down configuration but $S > S_{\mathrm{min}}$ exist in the intermediate range $r_{\mathrm{ud}-} < r < r_{\mathrm{ud}+}$, as shown by the dashed red line. These misaligned BHs have an infinite precessional period τ: they exponentially approach the up-down configuration on the precession time t_{pre} but never reach it.

The evolving relationship between the up-down configuration and the spin-orbit resonances parameterized by the angles θ_i is seen in Fig. 2. The solid curves show the $\Delta\Phi = 0$ resonances [$\xi_{\mathrm{min}}(J)$] for separations $10M \leq r \leq 3000M$, while the dashed curves show the $\Delta\Phi = \pi$ resonances [$\xi_{\mathrm{max}}(J)$]. The up-down configura-
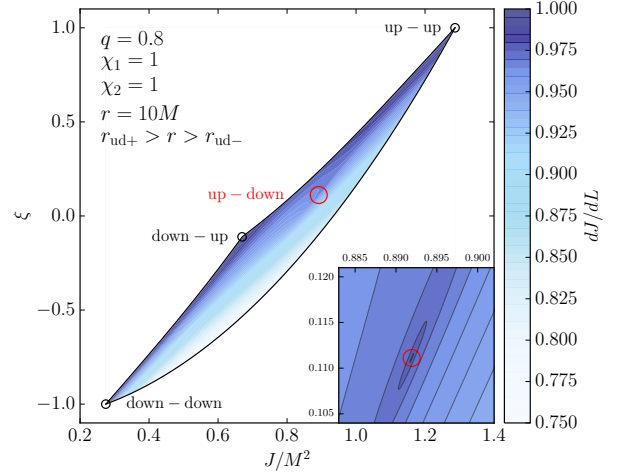
tion is located in the bottom right corner of this figure. For $r > r_{\mathrm{ud}+}$, the up-down configuration lies on the solid curves and belongs to the $\Delta\Phi = 0$ family, but for smaller separations these curves detach from the bottom right corner, and thus up-down is no longer a minimum of $\xi_\pm(S)$. The dashed curves indicating the $\Delta\Phi = \pi$ family migrate to the right with decreasing separation and reach the bottom right corner, making the up-down configuration a maximum of $\xi_\pm(S)$, for $r < r_{\mathrm{ud}-}$. The up-up and down-down configurations (top right and bottom left corners) belong to both resonant families, reflecting the degeneracy of the effective-potential loop as a single point that is both minimum and maximum. The down-up configuration (top left) always belongs to the $\Delta\Phi = \pi$ family and is thus a maximum ξ_{max}.

The stability of a system is determined by its response to perturbations, in this case to the spin angles $(\delta\theta_1, \delta\theta_2, \delta\Delta\Phi)$ or equivalently to the angular momenta $(\delta S, \delta J, \delta\xi)$. After such a perturbation, configurations that are extrema of $\xi_\pm(S)$ (all aligned configurations except up-down for $r_{\mathrm{ud}-} < r < r_{\mathrm{ud}+}$) will undergo oscillations in S (and thus the three spin angles) that are linear in the perturbation amplitude, and have a period τ that is independent of this amplitude. This is a stable response equivalent to that of a simple harmonic oscillator. The response of the up-down configuration for $r_{\mathrm{ud}-} < r < r_{\mathrm{ud}+}$ is very different, as seen in the middle panels of Fig. 1: S oscillates between the turning points $S_\pm$ independent of the perturbation amplitude, but the period τ of these oscillations – as predicted by Eq. (27)

of [37] – diverges logarithmically as this amplitude approaches zero. This is an unstable response: the time it takes for a zero-energy particle with $dx/dt < 0$ to travel from finite x_0 to δx in the unstable potential $V = -\frac{1}{2}kx^2$ similarly diverges logarithmically with δx.

A perturbative analysis of nearly aligned configurations [41] can identify that perturbations can oscillate at complex frequencies (indicating an instability) in the same region $r_{\rm ud-} < r < r_{\rm ud+}$ found here, but such analysis cannot predict the amplitude of these perturbations or their response to precession-averaged radiation reaction.

Radiation reaction. – We have shown that for $r_{\rm ud-} < r < r_{\rm ud+}$, spin configurations with J and ξ infinitesimally close to the up-down configuration can experience finite-amplitude oscillations in S and the angles θ_1, θ_2, and $\Delta\Phi$. We now investigate how these configurations evolve on the longer radiation-reaction time $t_{\rm RR}$. Since ξ is conserved throughout the inspiral and L monotonically decreases at 2.5PN order, the only challenge is to evolve J. In [36, 37] we derived a precession-averaged expression for dJ/dL, a contour plot of which is shown in Fig. 3. The shaded region shows the allowed values of J and ξ for this mass ratio, spin magnitudes, and binary separation. The spin-orbit resonances, being extrema of $\xi_\pm(S)$, constitute the boundaries of this region. The up-up, down-down, and down-up configurations, being spin-orbit resonances, lie on these boundaries. At $r_{\rm ud+}$, the up-down configuration detaches from the right boundary of this region [it stops being a minimum of $\xi_\pm(S)$] and begins to migrate leftwards through the allowed region, eventually reattaching to the left boundary at $r_{\rm ud-}$ [where it becomes a maximum of $\xi_\pm(S)$]. This is just an alternative visualization of the four panels of Fig. 1.

For all four aligned configurations, $\mathbf{J}$ and $\mathbf{L}$ are aligned so $dJ/dL = 1$ is maximized. However, the nature of these maxima is very different for the stable and unstable configurations. For the stable configurations, the partial derivatives of dJ/dL with respect to J and ξ remain finite, implying that neighboring points separated by $(\delta J, \delta\xi)$ slowly drift away at a rate that scales linearly with these infinitesimal quantities. The unstable configuration however is a cusp where these partial derivatives approach $\pm\infty$, depending on whether this point in the $J\xi$-plane is approached from below or above. Neighboring points (experiencing large-amplitude oscillations in S, as seen in the middle panels of Fig. 1) rapidly deviate from the up-down configuration as it sweeps across the allowed region. This is an essential point: even if the stability of the up-down configuration is restored in the PN regime ($r_{\rm ud-} > 10M$), radiation reaction during the inspiral between $r_{\rm ud\pm}$ will drive BHs initially in this configuration to large misalignments prior to merger. The migration of the up-down configuration through the $J\xi$-plane also reconciles the instability with the empirical result that isotropic spin distributions remain isotropic during the inspiral [19, 20]: although nearby binaries
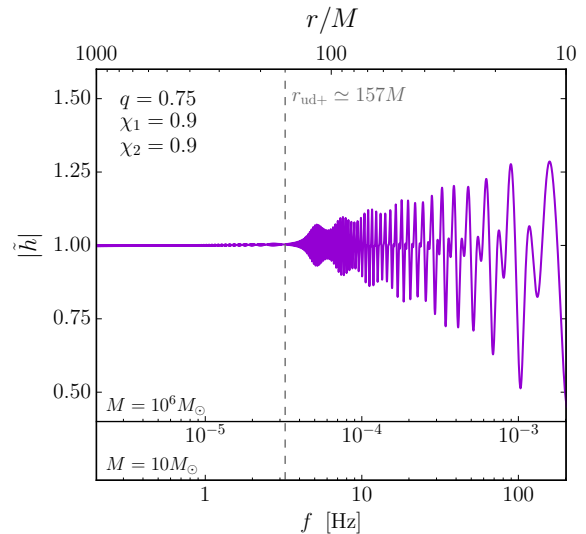

FIG. 4. Normalized GW Fourier amplitude $\tilde{h}$ (cf. Ref. [41]) as a function of orbital frequency f and binary separation r during the inspiral of BHs with $q = 0.75$ and $\chi_1 = \chi_2 = 0.9$. At the initial separation $r = 1000M$, the spins are nearly in the up-down configuration, but this configuration becomes unstable below $r_{ud+} \simeq 157M$, after which large precession-induced modulations occur at frequencies accessible to GW detectors.

may indeed be left behind, the unstable configuration will always encounter a fresh supply, until it is restored to stability at the left edge of the allowed region.

GW astronomy. – Binaries with separations in the unstable region between $r_{\rm ud\pm}$ emit GWs with frequencies in the range $f_{\rm ud\pm} \simeq 6.4 \times 10^4 {\rm Hz}(M/M_\odot)^{-1}(1-q)^3/(\sqrt{\chi_1} \pm \sqrt{q\chi_2})^6$, within or below the sensitivity band of existing and planned GW detectors [8–15]. In Fig. 4, we show the waveform of one such binary initially near the up-down configuration before entering the unstable region. Once the binary crosses the threshold at $r_{\rm ud+}$, its waveform develops large-amplitude precessional modulation on the precession time $t_{\rm pre}$. The amplitude of this modulation is independent of the initial deviation from the up-down configuration: it is set by the finite-amplitude oscillations in S seen in the middle panels of Fig. 1. Modulation occurs on two distinct timescales associated with the precession of $\mathbf{L}$ in a frame aligned with $\mathbf{J}$. In this frame the direction of $\mathbf{L}$ is specified by the polar angle $\cos\theta_L = \hat{\mathbf{L}}\cdot\hat{\mathbf{J}}$ and the azimuthal angle Φ_L in the plane perpendicular to $\mathbf{J}$. The longer of these timescales is τ (the period of oscillations in θ_L), while the shorter timescale is $(2\pi/\alpha)\tau$ (the precession-averaged time for Φ_L to change by 2π) [36, 37]. Measuring this modulation could yield insights into the astrophysical origins of binary BHs [18, 37]. Spin precession could also affect the electromagnetic counterparts to BH mergers [42, 43] and the probability of ejecting a supermassive BH from its host galaxy [30–32, 44]. We look forward to confronting these predictions with observations in the dawning age of GW astronomy.

* d.gerosa@damtp.cam.ac.uk
† kesden@utdallas.edu
‡ rossma@rit.edu
§ aklein@olemiss.edu
¶ eberti@olemiss.edu
** u.sperhake@damtp.cam.ac.uk
†† daniele.trifiro@ligo.org

[1] S. Bowyer, E. T. Byram, T. A. Chubb, and H. Friedman, Science **147**, 394 (1965).
[2] C. T. Bolton, Nature **235**, 271 (1972).
[3] B. L. Webster and P. Murdin, Nature **235**, 37 (1972).
[4] F. Hoyle and W. A. Fowler, MNRAS **125**, 169 (1963).
[5] D. Lynden-Bell, Nature **223**, 690 (1969).
[6] M. C. Begelman, R. D. Blandford, and M. J. Rees, Nature **287**, 307 (1980).
[7] P. C. Peters and J. Mathews, Physical Review **131**, 435 (1963).
[8] G. M. Harry and LIGO Scientific Collaboration, Classical and Quantum Gravity **27**, 084006 (2010).
[9] C. S. Unnikrishnan, International Journal of Modern Physics D **22**, 1341010 (2013).
[10] K. Somiya, Classical and Quantum Gravity **29**, 124007 (2012), arXiv:1111.7185 [gr-qc].
[11] M. Punturo *et al.*, Classical and Quantum Gravity **27**, 194002 (2010).
[12] R. N. Manchester and IPTA, Classical and Quantum Gravity **30**, 224010 (2013), arXiv:1309.7392.
[13] R. N. Manchester *et al.*, PASA **30**, e017 (2013), arXiv:1210.6130 [astro-ph.IM].
[14] F. Jenet *et al.*, ArXiv e-prints (2009), arXiv:0909.1058.
[15] M. Kramer and D. J. Champion, Classical and Quantum Gravity **30**, 224009 (2013).
[16] V. Kalogera, Astrophys.J. **541**, 319 (2000), arXiv:astro-ph/9911417.
[17] J. R. Hurley, C. A. Tout, and O. R. Pols, MNRAS **329**, 897 (2002), arXiv:astro-ph/0201220.
[18] D. Gerosa, M. Kesden, E. Berti, R. O'Shaughnessy, and U. Sperhake, Phys. Rev. D **87**, 104028 (2013), arXiv:1302.4442 [gr-qc].
[19] J. D. Schnittman, Phys. Rev. D **70**, 124020 (2004), astro-ph/0409174.
[20] T. Bogdanović, C. S. Reynolds, and M. C. Miller, ApJ **661**, L147 (2007), astro-ph/0703054.
[21] J. M. Bardeen and J. A. Petterson, Astrophys.J. **195**, L65 (1975).
[22] M. C. Miller and J. H. Krolik, ApJ **774**, 43 (2013), arXiv:1307.6569 [astro-ph.HE].
[23] D. Gerosa, B. Veronesi, G. Lodato, and G. Rosotti, MNRAS **451**, 3941 (2015), arXiv:1503.06807.
[24] A. R. King, S. H. Lubow, G. I. Ogilvie, and J. E. Pringle, MNRAS **363**, 49 (2005), astro-ph/0507098.
[25] B. M. Barker and R. F. O'Connell, General Relativity and Gravitation **11**, 149 (1979).
[26] K. S. Thorne and J. B. Hartle, Phys. Rev. D **31**, 1815 (1985).
[27] L. E. Kidder, Phys. Rev. D **52**, 821 (1995), gr-qc/9506022.
[28] T. A. Apostolatos, C. Cutler, G. J. Sussman, and K. S. Thorne, Phys. Rev. D **49**, 6274 (1994).
[29] C. Cutler and É. E. Flanagan, Phys. Rev. D **49**, 2658 (1994), gr-qc/9402014.
[30] J. A. González, M. Hannam, U. Sperhake, B. Brügmann, and S. Husa, Physical Review Letters **98**, 231101 (2007), gr-qc/0702052.
[31] M. Campanelli, C. O. Lousto, Y. Zlochower, and D. Merritt, Physical Review Letters **98**, 231102 (2007), gr-qc/0702133.
[32] M. Campanelli, C. Lousto, Y. Zlochower, and D. Merritt, ApJ **659**, L5 (2007), gr-qc/0701164.
[33] D. Merritt and R. D. Ekers, Science **297**, 1310 (2002), astro-ph/0208001.
[34] L. Á. Gergely and P. L. Biermann, ApJ **697**, 1621 (2009), arXiv:0704.1968.
[35] www.damtp.cam.ac.uk/user/dg438/spinprecession www.davidegerosa.com/spinprecession,.
[36] M. Kesden, D. Gerosa, R. O'Shaughnessy, E. Berti, and U. Sperhake, Physical Review Letters **114**, 081103 (2015), arXiv:1411.0674 [gr-qc].
[37] D. Gerosa, M. Kesden, U. Sperhake, E. Berti, and R. O'Shaughnessy, ArXiv e-prints (2015), arXiv:1506.03492 [gr-qc].
[38] T. Damour, Phys. Rev. D **64**, 124013 (2001), gr-qc/0103018.
[39] É. Racine, Phys. Rev. D **78**, 044021 (2008), arXiv:0803.1820 [gr-qc].
[40] M. Kesden, U. Sperhake, and E. Berti, Phys. Rev. D **81**, 084054 (2010), arXiv:1002.2643 [astro-ph.GA].
[41] A. Klein, N. Cornish, and N. Yunes, Phys. Rev. D **88**, 124015 (2013), arXiv:1305.1932 [gr-qc].
[42] M. Milosavljević and E. S. Phinney, ApJ **622**, L93 (2005), astro-ph/0410343.
[43] A. Loeb, Physical Review Letters **99**, 041103 (2007), astro-ph/0703722.
[44] M. Kesden, U. Sperhake, and E. Berti, ApJ **715**, 1006 (2010), arXiv:1003.4993 [astro-ph.CO].
[45] J. D. Hunter, Computing in Science and Engineering **9**, 90 (2007).